Multi-region lifetime assessment of reinforced concrete structures subjected to carbonation and climate change

Emilio Bastidas-Arteaga, G. Rianna, H. Gervasio, M. Nogal

Please cite this paper as:

Bastidas-Arteaga E, Rianna G, Gervasio H, Nogal M. (2022) Multi-region lifetime assessment of reinforced concrete structures subjected to carbonation and climate change. *Structures.*45(2022):886–99. https://doi.org/10.1016/j.istruc.2022.09.061

Multi-region lifetime assessment of reinforced concrete structures subjected to carbonation and climate change

E. Bastidas-Arteaga[a], G. Rianna[b], H. Gervasio[c1] and M. Nogal[d]

[a] *Laboratory of Engineering Sciences for the Environment (LaSIE - UMR CNRS 7356), La Rochelle University, La Rochelle, France*

[b] *REgional Model and geo-Hydrological Impacts, Centro Euro-Mediterraneo sui Cambiamenti Climatici, Italy*

[c] *ISISE, Departamento de Engenharia Civil, Universidade de Coimbra, Portugal*

[d] *Faculty of Civil Engineering and Geosciences, Delft University of Technology, the Netherlands*

ABSTRACT

The built environment is already and will be facing severe consequences related to climate change. Considering the durability of structures, the increase of carbon-dioxide (CO_2) concentration and changes on temperature and relative humidity may accelerate carbonation-induced corrosion, thus affecting the service life of reinforced concrete structures. Several studies have assessed the potential effects of climate change on concrete carbonation for specific locations, and this requires to convert climate databases, which come in various spatial resolutions, to scales that are suitable for the purpose of the study. However, there is not a consistent methodology for using climate projections databases at various spatial scales (e.g., city, district, region, country, etc.). Hence, the main goal of this research is to propose an approach allowing for multi-region assessment of carbonation of reinforced concrete structures, under changing climate. The proposed methodology is based on a carbonation model that takes into account the effects of climate change over time. Moreover, procedures and recommendations are provided to reduce errors in lifetime assessment, such as selection of climate change scenarios, choice of simulation chains, and bias correction. The use of the proposed approach is illustrated by computing carbonation depths for several places located in three districts in Portugal: Porto (north), Lisboa (Middle), and Faro (South). The overall results allow to conclude that: (i) specific climate conditions inside a district, namely temperature and relative humidity, modify the carbonation depths (e.g.: a variation of 19% was obtained for the carbonation depth in the district of Lisbon) ; (ii) bias-correction should be systematically carried out to avoid errors in the assessments (for example, in the district of Faro, the time to initiate corrosion was over estimated by about 7 years without bias correction); and (iii) climate change could accelerate concrete carbonation of structures in the different locations considered in Portugal (under the most pessimistic climate scenario, the time to corrosion initiation was below 100 years for all locations).

KEYWORDS: Reinforced concrete structures; Corrosion; Carbonation; CO_2 concentration; Climate Change; Atmospheric Reanalysis

[1] Corresponding author:

Helena Gervasio, Civil Engineering Department - University of Coimbra, Rua Luís Reis Santos - Polo II, 3030-788 Coimbra, PORTUGAL, Email: hger@dec.uc.pt

1 INTRODUCTION

As result of anthropic activities, CO_2 concentration is largely increasing at global scale, moving from about 315 ppm in Sixties up to about 415 ppm registered in the last years in the Mauna Loa station. As well known, the increase of atmospheric CO_2 and other climate altering gases induced an increase in global air temperature (about 1°C compared to the preindustrial era) (IPCC, 2021), while the evolutions in atmospheric humidity do not reveal clear trends, being heavily affected by local conditions (sea distance, orography, urban environment). Climate change is unequivocal, as clearly acknowledged by the United Nations Intergovernmental Panel on Climate Change (IPCC, 2021), and the built environment is already facing severe consequences from these changes (UKCIP, 2005; Wilby, 2007; Li et al., 2012; Bastidas-Arteaga, 2021).

Among the several investigated impacts, the forcing of global warming (increase on carbon-dioxide concentration) and the resulting changes on temperature and relative humidity under certain conditions may accelerate carbonation-induced corrosion, thus affecting the durability and serviceability of reinforced concrete structures (Yoon et al., 2007; Cole and Paterson, 2010; Larrard et al., 2014; Trivedi et al., 2014;).

The precise extent of such impact is uncertain as the main environmental drivers of carbonation-induced corrosion vary significantly from place to place and over time. However, how to obtain reliable projections of such variables, with an appropriate resolution, over the next 100 years? Moreover, how do these spatial and temporal variabilities affect the carbonation mechanisms in reinforced concrete structures, and reducing their service life? The answers to these questions are the main levers of this research work.

Many research works have investigated to which extent the service life of the reinforced concrete structures can be compromised in the context of a changing climate. Stewart et al. (2002) adopted a probabilistic model to assess temporal and spatial variability of CO_2 concentrations on carbonation of reinforced concrete structures. They concluded that CO_2 concentration in urban environments was about 5% to 10% higher than in rural environments; however, such increase had little influence on the predicted carbonation depths (it is noted that a climate change prediction of up to 450 ppm was considered for a service life up to 100 years). In a study carried out by Yoon et al. (2007), it was concluded that with increasing CO_2 concentrations, the progress of concrete carbonation was faster for concretes with higher w/c ratios. In a study focussing on Australia, it was predicted that by 2100, the damage due carbonation would increase up to 400% for inland and temperate climates (Stewart et al., 2011). Talukdar et al. (2012a) conducted a study in Canada to determine the influence of increasing temperature, duration of the hot season and concentration of CO_2 on the carbonation depth, obtaining increments of 45% when comparing the CO_2 levels in year 2000 with the strong increase expected not implementing mitigation strategies (A1F1 scenario) by 2100. Talukdar and Banthia (2013) analyzed the same scenarios but in this case only considered the effect of varying temperature at various locations, i.e., Mumbai, London, New York City, Sydney, Toronto and Vancouver. They observed a large variation in the results, obtaining increments of carbonation depths between 15 mm (27%) and 35 mm (45%). Saha and Eckelman (2014) analysed carbonation in the Boston metropolitan area considering increasing temperatures and CO_2 concentrations. They observed an increment of the carbonation depths of 40% when comparing the two same scenarios.

In addition to temperature and CO_2 concentration, variable relative humidity was introduced by Larrard et al. (2014) in the assessment of carbonation effects for different cities in France, under different climate change scenarios. It was concluded that climate change and local relative humidity had a significant impact on the durability of reinforced concrete structures. The variability of relative humidity was also considered by Peng and Stewart (2014) in a study about the carbonation depths in China. They concluded increments of 45% when compared the CO_2 levels in year 2000 and 2100 under an updated no mitigation scenario (Representative Concentration Pathway, RCP8.5 scenario). Much larger values were obtained by Chen et al (2021) in three locations in China, i.e., Qingdao, Harbin and Ningbo, when applying a new combined carbonation model based on experimental results that includes variable temperature, RH and CO_2 concentrations. The variation with time assessed for these parameters is also considered by AL-Ameeri et al (2021) in the London case, obtaining increments up to 88% when compared RCP8.5 scenario in 2100 in relation to the reference scenario of constant CO_2 levels of 400 ppm (comparable to the present value). In the most vulnerable location, they estimated an increment of the carbonation depth of 345% under the RCP8.5 scenario in 2100 in relation to 2020. Mizzi et al. (2018) analysed the effect of using different concrete

grades in structures in Malta and compared the carbonation depths for the RCP2.6 (associated to the adoption of significant mitigation strategies at global scale) and RCP8.5 scenarios between 2020 and 2070 with consideration of increasing CO_2 concentration and temperatures. The increment of carbonation depths varied linearly from 18.5 mm to 9.3 mm associated with concrete grades C15 to C45, respectively, and Ekolu (2020) concluded that the effect of carbonation was negligible for concrete with strengths larger or equal than 40 MPa, whereas for lower quality concretes, carbonation depth increase can reach 31% by 2100 under RCP8.5 compared to 2000. These conclusions were based on the application of a natural carbonation prediction model that incorporates variable temperature and CO_2 concentrations in two cities of South Africa, Johannesburg and Durban.

Previous studies shown that climate change will definitively modify concrete carbonation patterns in the upcoming years. However, it is noted that most works adopted a simplified approach for climate projections. For instance, in some cases a time-invariant (constant) CO_2 concentration is assumed (e.g.; Sudret et al. 2007); in other cases, a linear grow of CO_2 concentration is considered for the time span of 100 years (e.g.: fib, 2006), or a future CO_2 concentration is assumed (e.g.: Stewart et al., 2002). Moreover, all the reviewed work focused on modeling the potential impact of climate change on carbonation-induced corrosion, rather than on the method to obtain reliable projections over time of the main drivers of such phenomenon, namely, atmospheric CO_2 concentration, local temperature and local relative humidity.

Currently, there is not a consistent and unified methodology to use climate change projections when studying climate change at various spatial scales (e.g., city, district, region, country, etc.), and this is of utmost importance for accurate predictions of carbonation-induced corrosion.

Within this context, the main goal of this research work is to provide a consistent approach for multi-region reliable assessment of future projections of climate forcing regulating the lifetime of concrete structures subjected to concrete carbonation.

Climate projections will be performed based on Global Climate Models (GCMs), which have usually horizontal resolutions with a grid size of about 50-100 km. This resolution is not considered adequate in case of the estimation of climate variability at the regional and/or local level (Oreskes et al, 2010). In this case, downscaling is required to analyze the local consequences of the global change. Downscaling can be performed by different methodologies but, in the proposed approach, the adopted procedure relies on the exploitation of Regional Climate Models (RCMs) obtained by dynamic downscaling, which have typically a horizontal resolution in the range of 10-25 km (USAID, 2014).

In spite of improved representation of atmospheric dynamics, data provided from such simulation chains are affected by errors due to spatial resolution, and prevent the adoption of raw outputs as forcing for impact models. To cope with such biases and permitting the adoption of the outputs of climate simulation chains as inputs to the impact models, a statistical technique, usually known as bias correction, will be adopted.

Hence, the proposed approach provides procedures and recommendations to reduce errors in lifetime assessment: selection of climate change scenarios, choice of simulation chains, and bias correction. Furthermore, the approach is applied to a case study, which entails the estimation of the carbonation depth of reinforced concrete structures in three distinct regions in Portugal, based on historic climatic characteristics and future climatic protections for such regions. It is noted that the three different regions may be considered as representative of the temperate climate in southern Europe.

In summary, the main novelties in this paper are:

- To provide a consistent approach for allowing to assess the regional variability in atmospheric forcing induced variations in carbonation depth, based on reliable climate projections over a period of 100 years;
- To show the need to consider regional variability in the assessment of the carbonation depth of reinforced concrete structures;
- To highlight the importance of using bias corrected climate data instead of raw data;
- To determine the expected climatic trends for the future decades in Portugal, and to show how they affect carbonation-induced corrosion of reinforced concrete structures in different locations.

Hence, the paper is organized as follows: the following section (section 2) describes the approach for multi-regional climate projections; section 3 presents the process of carbonation-induced corrosion, and the adopted model for the estimation of the carbonation depth. The climate variables driving this deterioration process are analyzed and discussed in section 4 in the present context of climate change. The proposed approach is illustrated and discussed in section 5 to analyze the Portuguese case study. Finally, conclusions and further work are drawn in section 6.

2 APPROACH FOR MULTI-REGION CLIMATE CHANGE ASSESSMENT

Representative Concentration Pathways (RCPs) provide the expected trends in Greenhouse Gases (GHG) concentration based on different assumptions related to socio-economic, demographic, and technological developments at global and regional scales. These are used as direct forcing in climate models. Specifically, in the context of Coupled Model Intercomparison Project 5 (CMIP5), four pathways are assumed as references and named according to the expected consequent increase in radiative forcing in the year 2100 relative to the pre-industrial era (1765): +2.6, +4.5, +6.0 and +8.5 W/m^2. Then, RCP2.6 represents an ambitious scenario in terms of climate mitigation policies (potentially, the only one able to address the increase in global temperature lower than 2°C) while RCP8.5 is the worst-case scenario representing the 90th percentile of no-policy baseline scenarios (van Vuuren et al., 2011).

Forced by RCPs, Global Climate Models (GCMs) and/or the most advanced and complex Earth System Models (ESMs with an explicit representations of biogeochemical processes) permit the numerical representation of the climate system in terms of physical, chemical, and biological features and interactions. In recent decades, the considerable progresses in climate modelling made possible by the increased computing power permitted a much finer (up to 50-100 km) and better representation of the global atmospheric dynamics (Breugem, 2007; IPCC, 2014). However, despite such improvements, these models are not adequate for assessments at the local/regional level for which the features of the area (distance from the sea, topography) play a key role (even with respect of large-scale atmospheric circulation). Under such constraints, dynamical downscaling by exploiting Regional Climate Models (RCMs) have been widely adopted. RCMs are numerical climate models covering a limited area at higher resolution (in the order of 10-25 km but with experiments up to 1-2 km) and nested for the area of interest on the global model from which they draw the boundary conditions. These allow a better resolution of the orography and permit solving a substantial fraction of the local atmospheric phenomena. A way to explore some of the main sources of uncertainty (Sanderson and Knutti, 2012; Wilby and Dessai, 2010) related to the imperfect knowledge of the climate system (model uncertainty) and about the socio-economic and technological developments (scenario uncertainty) is represented by the adoption of multi-model ensembles (MME) defined as a set of simulations from different models over a common domain with spatial resolutions. They are usually considered “ensembles of opportunity” (Tebaldi and Knutti, 2007) where the participation is related to the voluntary participation of the different research institutions. In this regard, MMEs cannot sample the uncertainties in systematic way and the spread of MME should be viewed as “lower bound on response uncertainty” (Parker, 2013). Despite the substantial improvement in representation of regional atmospheric patterns associated to the use of RCMs, biases of varying entities depending on the area and the weather variables of interest, can hamper the use of raw climate data as input for impact analysis. To overcome this issue, different approaches, known as Bias Correction (BC) methods, have been proposed in recent years (Maraun, 2016; Maraun et al., 2017). They can be defined as “all methods that calibrate an empirical transfer function between simulated and observed distributional parameters and apply this transfer function to output simulated by the considered model” (Maraun, 2016).

Hence, the proposed approach aims at providing reliable databases for comprehensive lifetime assessment of buildings and infrastructure assets when considering their spatial distribution at different scales (country, region, and sub-region). This approach will be applied to a Portuguese case study, to assess the regional variability of concrete carbonation under changing climate; however, it could be applied for studying other deterioration processes and/or locations. It consists of the following main steps:

- *Define the scale of the analysis*: the Portuguese case study considers three main climate regions and several points (cities) in each region (section 4).

- *Select the climate change scenarios*: A multi-scenario analysis allows to estimate the more optimistic and pessimistic assessment. In the present paper three RCPs are considered: RCP2.6, RCP4.5 and RCP8.5 that could be considered as optimistic, mid-way, and pessimistic scenarios.
- *Define the simulation chains*: This step allows to consider information coming from several climate models. The spatial resolution of the data is a key aspect to get reliable projections. Therefore, it is suggested to consider downscaled data with a resolution close to 10km that could be able to retrieve the climate conditions for a local context. Two climate simulation chains are selected herein among those made available within the EURO-CORDEX initiative (Coppola et al., 2021; Jacob et al., 2020) with a spatial resolution of 0.11° (Table 1). Of course, they cannot provide comprehensive information about the spread associated to the future trends of weather variables of interest over the selected area, but they support the illustration of the proposed approach providing first insights about how the findings could be influenced by the climate simulation chains.

Table 1: Climate simulation chains considered for the study

Driving GCM[2]	RCM	LABEL
ICHEC-EC-EARTH	SMHI-RCA4 (Sweden)	ICHEC-RCA4
MPI-M-MPI-ESM-LR	SMHI-RCA4 (Sweden)	MPI-RCA4

- *Perform bias correction*: Bias correction allows to refine the data previously defined. The importance of this step will be illustrated in the case study. The approach adopted for bias correction is Scaled Distribution Mapping (Switanek et al., 2017); it is an explicitly trend-preserving method. Monthly observed distribution is scaled by the variations returned by the model between future and current reference distributions and by the likelihood of the events. It requires defining a priori a statistical distribution for the weather variable of interest (e.g., Normal for temperature, Gamma for precipitation). Before scaling, temperature values are detrended; after scaling, the bias adjusted values are reordered and the trend is added again. Casanueva et al. (2020) displayed the good performances of the SDM approach in preserving the trends returned by the original raw climate simulation subject to bias correction for different indices and variables considered (also not preserved by construction). In this regard, it is intended that trend-preserving methods should be preferred if there are no specific physical arguments justifying the need for a modification (Dosio, 2016).

3 CARBONATION-INDUCED CORROSION

In presence of CO_2, the calcium-baring phases of concrete transform into calcium carbonate, causing a decrease of concrete alkalinity. Carbonation is measured in terms of the average distance from the surface of the concrete affected by reduced alkalinity. When the so-called carbonation-depth reaches the rebar level, the pH values below the steel passivation threshold make steel vulnerable to corrosion. The corrosion initiation stage, characterized by the carbonation penetration, dominates the service life of reinforced concrete structures. Once that the carbonation depth reaches the rebar level, the corrosion propagation stage starts, leading to a rapid structural degradation. The rate of carbonation depends on several variables: some external such as the temperature, environmental humidity and CO_2 levels, other ones related to the structural element such as the diffusion coefficient, cement content, amount of calcium oxide in cement and water-cement ratio.

Concrete carbonation models provide the evolution in time of the carbonation depth $x_c(t)$ (in cm). Advanced numerical concrete carbonation models are found in the literature (Ravahatra et al., 2019, Londhe et al., 2021). Since this study focuses on quality and regional variability of climate databases, we use the concrete

[2] Equilibrium Climate Sensitivity, the hypothetical value of global warming at equilibrium for a doubling of CO2, is respectively equal to 3.3 °C and 3.6°C for ICHEC-EC-EARTH and MPI-M-MPI-ESM-LR. They are quite close to the multi-model ensemble value (3.2°C) estimated for CMIP5 simulations (Wyser et al., 2020; Meehl et al., 2020)

carbonation model described in this section that allows to consider temporal variations of CO_2 concentration, temperature and relative humidity due to climate change. In this model the carbonation depth is estimated as (Duracrete, 2000; Stewart et al., 2011; Yoon et al., 2007):

$$x_c(t) = \sqrt{\frac{2D_1(t)^{-n_d}}{a} C_{CO_2} t} \left(\frac{t_0}{t}\right)^{n_m} \quad (1)$$

where D_1 is the CO_2 diffusion coefficient obtained at time $t_0 = 1$ year; n_d is the ageing factor for D_1; C_{CO_2} is the mass concentration of CO_2 in the environment (10^{-3} kg/m^3); n_m is a factor to account for the exposure to microclimatic wetting and drying cycles ($n_m = 0$ for sheltered outdoor and $n_m = 0.12$ for unsheltered outdoor); and a is estimated as (Duracrete, 2000; Stewart et al., 2011; Yoon et al., 2007):

$$a = 0.75 C_e C_a O \alpha_H \frac{M_{CO_2}}{M_{C_aO}} \quad (2)$$

where C_e is the cement content (kg/m^3); C_aO is the C_aO content in the cement (~0.65); M_{CO_2} and M_{C_aO} are respectively the molar masses of CO_2 (44 g/mol) and C_aO (56 g/mol); and α_H is a degree of hydration that could be estimated as a function of the water to cement ratio (w/c) (de Larrard, 1999):

$$\alpha_H \approx 1 - e^{-3.38 w/c} \quad (3)$$

Stewart et al., (2011) modified Equation (1) to account for the effects of climate change as follows:

$$x_c(t) = \sqrt{\frac{2k_{site}D_1(t)^{-n_d}}{a} \int f_T(t) f_{RH}(t) C_{CO_2}(t) dt} \left(\frac{t_0}{t}\right)^{n_m} \quad (4)$$

where k_{site} is a factor that accounts for the potential increase of CO_2 concentration in urban or industrial areas; $C_{CO_2}(t)$ accounts for the time-variant increase of CO_2 concertation for a given climate change scenario; and $f_T(t)$ and $f_{RH}(t)$ are factors to account respectively for the effects of time-variant temperature and relative humidity on the carbonation process. The effect of a time-variant temperature ($T(t)$ in K) is modelled based on the Arrhenius law (Duracrete, 2000; Yoon et al., 2007) for a reference temperature $T_{ref} = 20$ºC:

$$f_T(t) = \exp\left(\frac{E}{R}\left[\frac{1}{T_{ref}} - \frac{1}{T(t)}\right]\right) \quad (5)$$

where E is the activation energy of the diffusion process (32 to 44.6 kJ/mol for ordinary Portland cements (Page et al., 1981) and R is the gas constant (8.314x10^{-3} kJ/mol·K). The effects of temperature variations on f_T are illustrated in Figure 1. It is noted that for several values of E the CO_2 diffusivity will increase for higher temperatures because f_T multiplies the CO_2 diffusion coefficient in Equation (4) (Figure 1a). Therefore, carbonation rates will increase for higher temperatures. The effect is larger when E increases.

The effect of a time-variant relative humidity, $RH(t)$, is estimated with respect to a reference relative humidity, $RH_{ref} = 0.65$, by using the following equation (fib, 2006; Schiessl et al., 2005; Stewart et al., 2011):

$$f_{RH}(t) = \begin{cases} 0 & \text{If } RH(t) \leq 0.25 \\ \left(\dfrac{1 - RH(t)^{f_e}}{1 - RH_{ref}^{f_e}}\right)^{g_e} & \text{Otherwise} \end{cases} \quad (6)$$

where f_e and g_e are parameters independent of exposure conditions and were determined from curve fitting –i.e., $f_e = 2.5$ and $g_e = 5$. In Figure 1b is observer that larger carbonation rates could be expected when the relative humidity is in the range [0.25, 0.65]. A decrease of the carbonation rate is expected when the relative humidity is larger than 0.65. Therefore, climate change could increase/decrease carbonation rates depending on future values for given scenarios and the initial relative humidity.

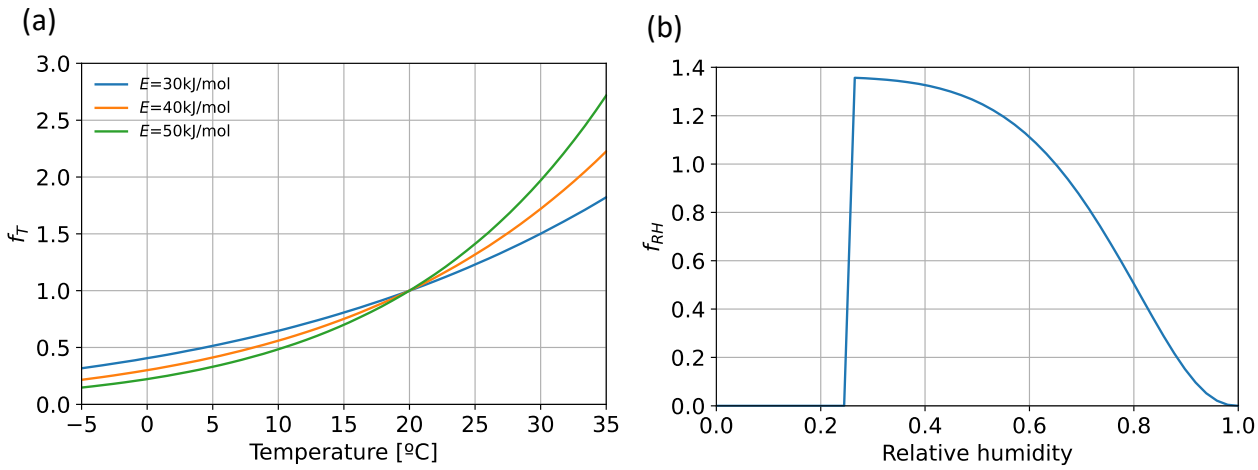

Figure 1: Effect of temperature and relative humidity variations on: (a) f_T and (b) f_{RH}

4 VARIABLES DRIVEN CARBONATION-INDUCED CORROSION AND CLIMATE CHANGE

4.1 Selected locations in Portugal

To assess the effects of the regional variability of climate parameters in the estimation of the carbonation depth of reinforced concrete structures, three different locations in Portugal were selected, as described in the following paragraphs.

The climate in Portugal is greatly influenced by the latitude, by the orography of the terrain and by the proximity to the Atlantic Ocean. According to the Portuguese Institute of Sea and Atmosphere (IPMA, 2022), in the period 1961-90, the average annual temperature varied between 7°C, in the highlands of the northern and central interior regions, and about 18°C, on the southern coast. Based on the same data, the average annual precipitation had the highest value in northern coastal region and the lowest value in the interior of the southern region.

For this study, three main areas were selected, as illustrated in Figure 2, with distinct climate characteristics: one in the northern area (Porto district, Figure 2b), one in the central part (Lisbon district, Figure 2c) and one in the southern area of the country (Faro district, Figure 2d).

For each district, different locations (grid points) were considered, as indicated in Figures 2b to 2d by the black stars. Hence, in the district of Porto, 4 locations were considered: Matosinhos, Póvoa do Varzim, Vila Nova de Gaia and Amarante. In the district of Lisbon, 5 locations were taken into account: Lisboa, Oeiras, Vila Franca de Xira, Azambuja and Lourinhã; and finally, in the district of Faro, 4 locations were considered: Faro, Tunes, V.R.S. Antonio and Alcoutim. Moreover, in each district, a reference location (reference grid point) was considered for comparison with the other locations. The reference grid point in each district is indicated by the character *R* next to the black star in Figures 2b to 2d, and those locations are Vila Nova de Gaia, Vila Franca de Xira and Alcoutim, in the districts of Porto, Lisbon and Faro, respectively.

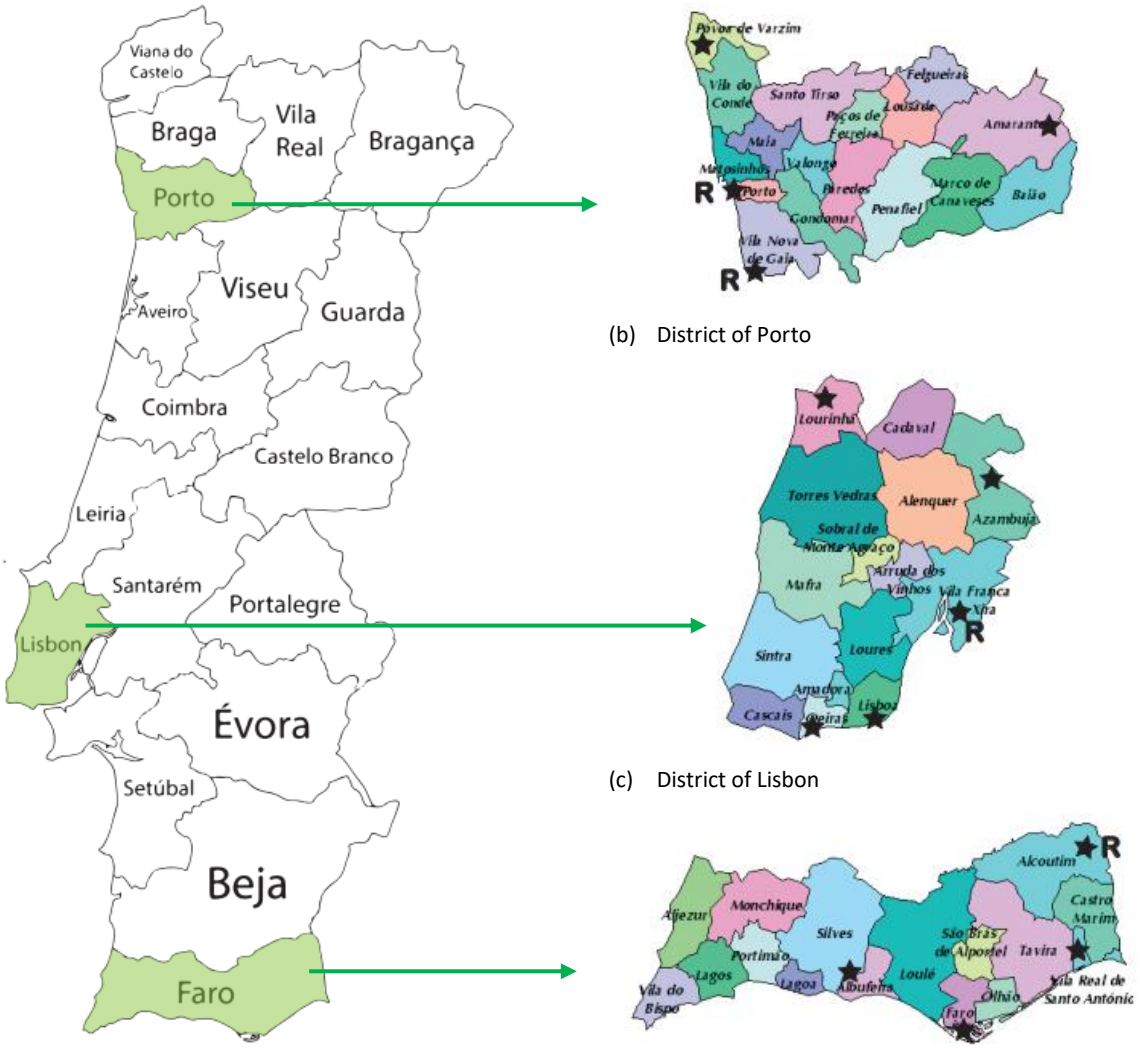

(a) Portugal mainland

(b) District of Porto

(c) District of Lisbon

(d) District of Faro (Algarve)

Figure 2: Selected locations in Portugal

The three locations have also distinct characteristics in terms of main economic activities and therefore, also in terms of respective emissions. Hence, taking into account the emission of Green House Gases (GHG), the emissions for the three reference grid points are provided in Table 2. The main source of GHG emissions in Vila Nova de Gaia is the sector of Transports, followed by the sector of Industry & electricity. In Vila Franca de Xira, the main source of GHG is the sector Industry & electricity, followed by the sector of Transports. In Alcoutim, the main source of GHG emissions is due to the sector of Agriculture. These emissions show that the two former locations are mainly urban areas; whereas, Alcoutim, is mainly a rural area. Therefore, different values of k_{site} (Equation (4)) are considered for each district to account for this specificity, as indicated in Table 2.

Table 2 GHG emissions in different locations expressed in Kton CO_2 equivalent (APA, 2021)

	Vila Nova Gaia (district of Porto)			Vila Franca Xira (district of Lisbon)			Alcoutim (district of Faro)		
Sector	**2015**	**2017**	**Diff**	**2015**	**2017**	**Diff**	**2015**	**2017**	**Diff**
Industry & electricity	375	336	-39.73	1375	1361	-13.81	3	1	-1.73
Residential & Services	34	61	26.79	45	50	4.74	1	1	-0.08
Transports	601	626	25.80	275	289	13.76	2	2	-0.04
Waste	69	67	-1.42	139	121	-18.19	1	1	-0.13
Agriculture	3	3	0.03	33	32	-0.49	6	6	-0.25
Forest fires	0	5	4.31	-	-		-	-	
	1082	1098	1.5%	1867	1853	-0.7%	13	11	-16.6%

4.2 Historic and future climate conditions

The analysis of climatic conditions considers two different time spans: historic/current period (1981-2020) and future periods since 1981 up to 2100. In both cases, the values provided in the following sub-sections are relative to the reference grid point in each selected district (see Figure 2).

4.2.1 Data for the current period

For the present period, time series are provided by ERA5-land (Muñoz-Sabater, 2019) reanalysis with a spatial resolution of about 9 km (0.1°). In general terms, a reanalysis "delivers a complete and consistent picture of the past weather" (https://youtu.be/FAGobvUGl24) by exploiting a single consistent numerical weather prediction model assimilating historical observations provided by different sources (satellite, in situ, multiple variables) but not homogeneously distributed around the globe. While weather prediction models use data assimilation only as initial condition, climate reanalysis can assimilate observations during the entire period. In this regard, ERA5 (Hersbach et al., 2019; Bell et al., 2020) represents the fifth generation of reanalysis developed by European Centre for Medium-Range Weather Forecasts (ECMWF) with global coverage and a spatial resolution of about 31 km; it covers the period since 1950 up to now with a latency of 5 days (outputs available at hourly scale). Compared to the previous generation (Dee et al., 2011), it relies on a finer resolution (~ 31 vs ~ 80 km) and substantial improvements in model physics, parametrization, Furthermore, in ERA5 land, enhanced resolution reanalysis data are made available over land by replaying the original land component of ERA5 with a version at the finer resolution of 9 km. ERA5 land exploits atmospheric forcing (e.g., air temperature, air humidity and pressure) from ERA5 atmospheric variables but accounting for the improved representation of the orographic features ("lapse rate correction"). Although the remarkable improvements in model physics and spatial resolution, ERA5 land should not be intended as a replacement of site-specific weather station observations. However, it can provide area-average data and an assessment of spatial variability whose reliability is strictly related to the number and quality of observations that could be assimilated on the area. It is worth recalling that ERA 5 land does not adopt explicit parametrizations for urban environment; then, specific dynamics (e.g. Urban Heat Island effect) could be not properly reproduced.

In Figure 3, mean monthly values of air temperature and relative humidity over 1981-2020 for the three districts are reported. Specifically, median value (continuous line), 10^{th} and 90^{th} percentiles (dashed lines) are computed among all the grid points included in the three different districts. Moreover, purple lines identify the reference grid points (R with stars in Figure 2)

For the three districts, the temperature patterns present the highest values during the summer season (June-July-August, JJA) and the lowest values during winter (December-January-February, DJF). Consequently, relative humidity patterns display minimum values during the Summer for the district of Porto, the median yearly value of temperature is estimated about equal to 14°C (13.7°C). Within the district (data not displayed), increasing temperature values can be retrieved moving from internal areas to the coastal areas with a variation slightly larger than 3°C between the "warmest" and the "coldest" grid points. For what concerns relative humidity, at annual scale, the median value is about equal to 0.76 while a weak increasing gradient is recognized from internal areas to the coastal ones due to the influence of the Atlantic Ocean (the difference between the "wettest" and the "driest" grid points is about 0.03).

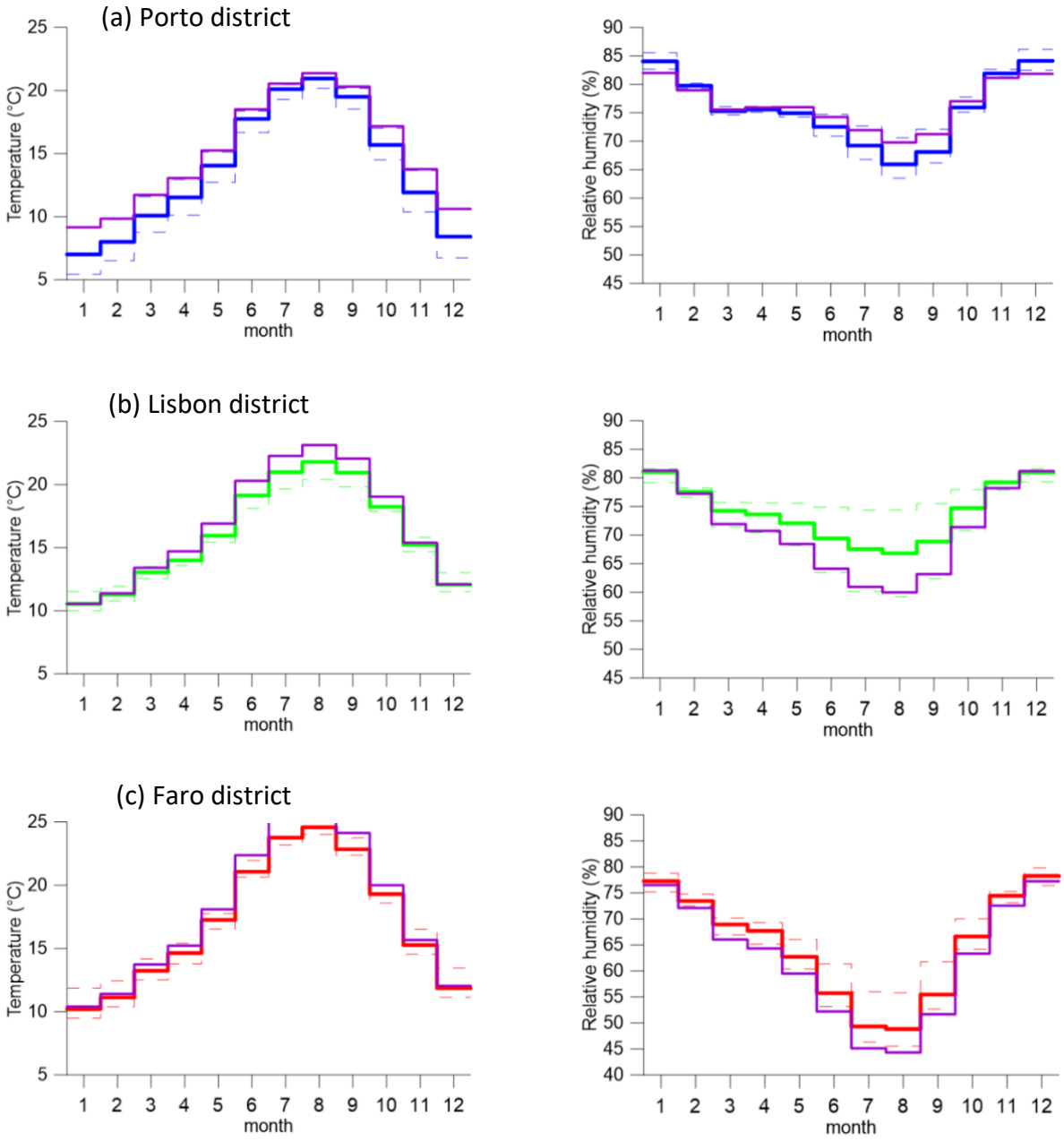

Figure 3: Monthly mean values of air temperature (left column) and relative humidity (right column) for (a) Porto, (b) Lisbon, and (c) Faro districts. Values are provided in terms of spatial median value (bold line), 10th and 90th percentiles (dashed lines). Purple lines identify mean values related to the reference grid points used to assess expected future changes.

For what concerns the district of Lisbon, the median yearly value of air temperature is about 16°C. Over the area, a clear decreasing trend can be recognized moving from the internal, southernmost areas to the coastal-northernmost ones (the difference, at annual scale, between the warmest and coldest grid points is about 1.5°C). In terms of relative humidity, the median value is about 0.74 with increasing values moving towards colder (North) and wetter (coastal) areas; in this case, the difference is about equal to 10%. About the reference grid point for future assessments, it is selected in the internal/southernmost areas which justifies the returned trends.

Finally, for the district of Faro, the median yearly value of air temperature slightly exceeds 17°C. Over the area, higher values of temperature are estimated in internal and southernmost areas (located on the coast) while the lowest values are returned for the areas located on Western coast (the spread between the warmest and coldest grid points is about 1.7°C). In terms of relative humidity, the median yearly value is about 0.65 with clear increasing gradients moving from the internal to the coastal areas. In this case, the reference grid point is positioned in the internal/northernmost part of the investigated region. It justifies the high values of temperatures and, at the same time, low relative humidity values.

4.2.2 *Data for future period and bias correction*

The second set of analyses is aimed at providing assessments about future trends of air temperature and relative humidity, using the approach described in section 2.

The time series from the historic period (1981) to the end of the XXI century are provided adopting a simulation chain widely consolidated in the scientific literature. One of its key elements are Representative Concentration Pathways (RCPs). The global trends in CO_2 for the historic period as returned by global (up to 2005) monitoring networks and for RCP-2.6, -4.5 and -8.5 scenarios up to 2100, as provided by Integrated Assessment Models (IAMs) reported in Figure 4. Furthermore, yearly values provided by the reference Portuguese observation site (1979-2020) located in Terceira Island (38.7660° N; 27.375° W), in Azores, and by the observation site located nearest to the pilot areas in Spain (2009-2020; Centro de Investigacion de la Baja Atmosfera; 41.8100° N; 4.93° West), are also provided in Figure 4. For the National observation sites, the years that were considered are only the ones where, at least, 8 monthly values were provided.

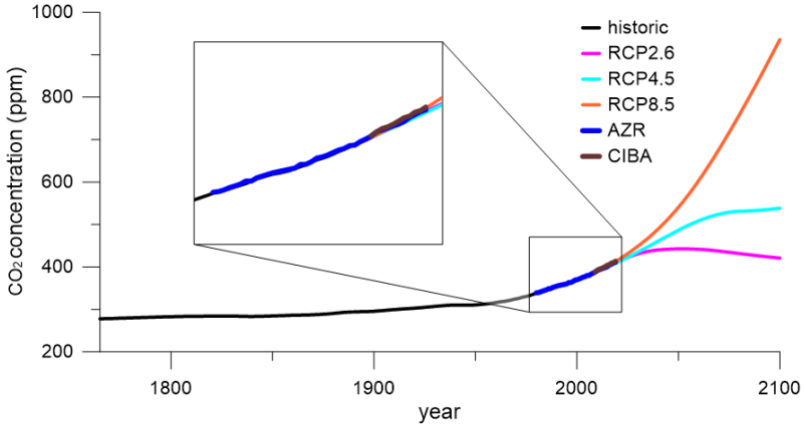

Figure 4: Evolution of CO_2 concentration as monitored or assessed at global scale (black line from 1765 to 2005); future scenarios under RCP2.6, RCP4.5 and RCP8.5. Yearly values provided by Portuguese observation site (AZR) and Valladolid (CIBA) are also provided.

Taking into account three RCPs (RCP2.6, RCP4.5 and RCP8.5) and the two climate simulation chains indicated in Table 1, in the following paragraphs, observed data is compared with raw and bias corrected data. As already referred, the approach adopted for bias correction is Scaled Distribution Mapping. Hence, in Figure 5, for the Porto reference grid point, the comparison between ERA5 land data (assumed as reference), raw and bias corrected data for the two climate simulation chains (CSCs) is displayed for temperature and relative humidity over the period 1981-2010.

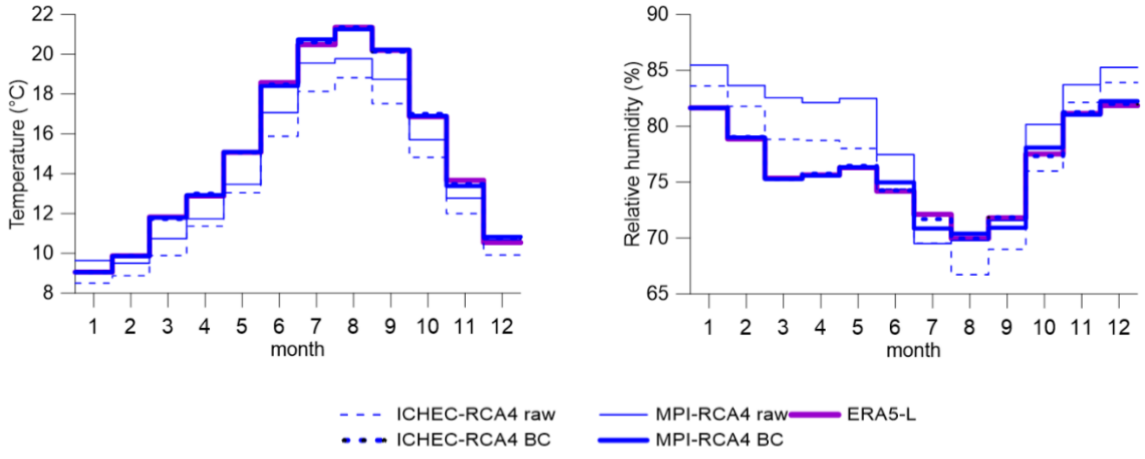

Figure 5: For Porto reference grid point, comparison of monthly mean values between ERA5 land (purple), ICHEC-EC-EARTH driven CSC raw (dashed thin blue) and BC (dashed thick blue) and MPI-M-MPI-ESM-LR raw (continuous thin blue) and BC (continuous thick blue). Reference period 1981-2010.

It is noted that the global climate models included in CMIP5 are forced by using observed values of climate altering gases concentration up to 2005. For the period 2006-2010, RCP8.5 is used as forcing. Nevertheless, very slight differences can be retrieved among the three scenarios in the first years (Figure 6). The enhancement related to the adoption of bias correction approach clearly arise; for ICHEC-RCA4, the mean absolute error computes for the monthly values reduces from about 1.7°C to about 0.1°C while, for MPI-RCA4, bias adjusting permits a reduction from about 1°C to about 0.1°C. The findings in terms of relative humidity (%) are quite similar: the mean absolute error moves from about 2% (3.6%) to about 0.1% (0.3%) for ICHEC-RCA4 (MPI-RCA4). Similar results (data not displayed) are found for the other two locations.

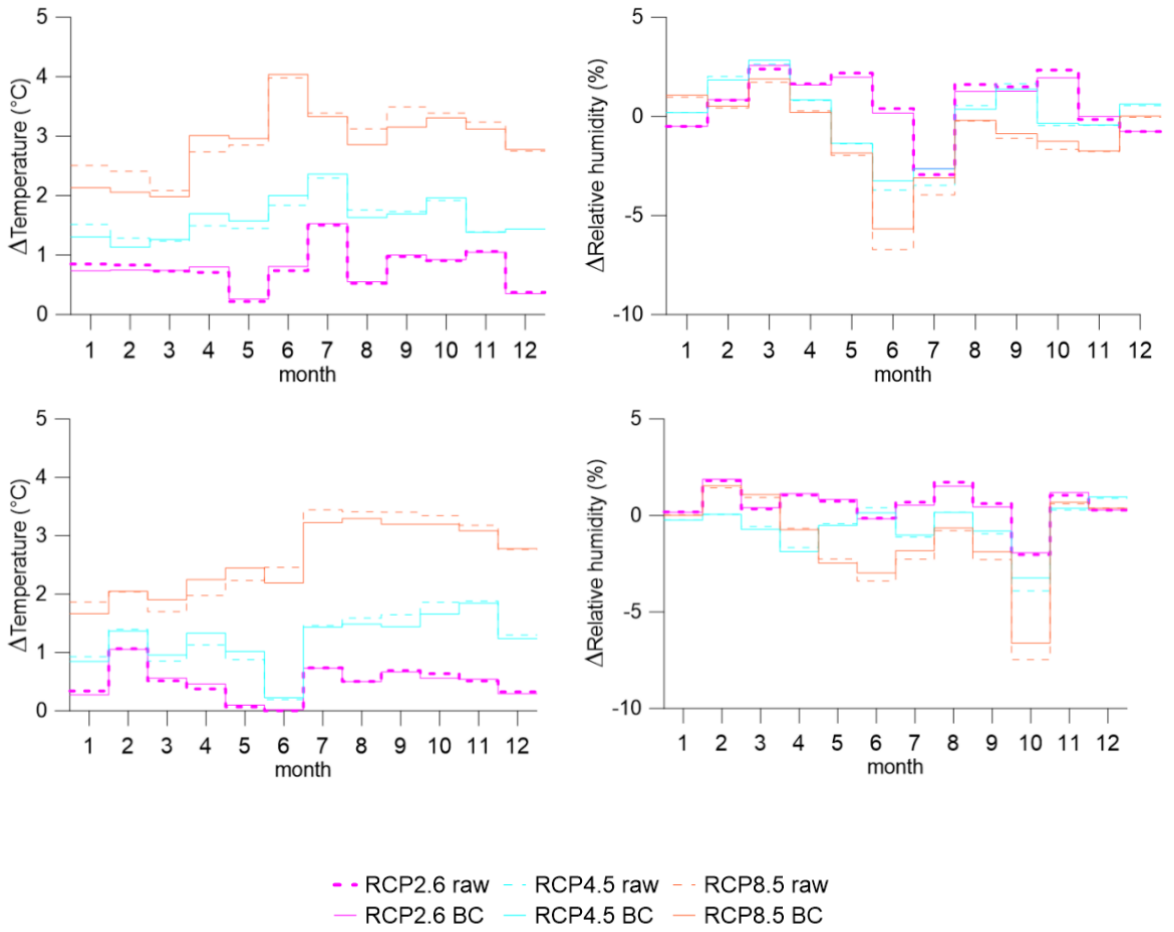

Figure 6: For Porto reference grid point, climate anomalies between the period 2071-2100 and the reference period 1981-2010 under RCP2.6 (magenta), RCP4.5(cyan), RCP8.5(orange) as returned by CSCs raw (dashed line) and BC (continuous line); for ICHEC-RCA4 (first row) and MPI-RCA4 (second row); for temperature (first column) and relative humidity (second column)

For Porto test case, Figure 6 reports the anomalies returned by comparing mean monthly temperature and relative humidity values for the two CSCs (raw and after bias correction). The first element to stress is the high capability of SDM method to preserve the trend evaluated by raw models; satisfying results are found regardless of considered variable, RCP or CSC. Moreover, in terms of temperature anomalies, an increase is expected under all the RCPs; nonetheless, it results main function of the RCP severity.

Considering bias-adjusted values, for ICHEC-RCA4, the mean yearly temperature anomaly is about 0.8°C (maximum 1.5°C in July), 1.6°C (maximum 2.4°C in July) and about 3°C (maximum 4°C in June) respectively under RCP-2.6, -4.5 and -8.5 scenarios. On the other side, for MPI-RCA4, the mean increase does not exceed 0.5°C (maximum 1.1° in February) under RCP2.6; 1.2°C (max 1.8°C in November) under RCP4.5 and 2.6°C (maximum 3.3°C in August) for RCP8.5. For what concern relative humidity, less clear and significant trends can be identified; for example, adopting ICHEC-RCA4, the mean yearly variation is about 0.6% with values ranging between -2.6% and 2.6% under RCP2.6. Under RCP4.5, the net variation is about equal to zero at yearly scale with variations between -3.3% and 3%. Finally, under RCP8.5, the expected yearly decrease does

not exceed 1% with larger decreases in the summer season probably associated to the higher temperature increases (about -6%). When MPI-RCA4 bias corrected values are considered, similar anomalies are returned: under RCP2.6 the increase is about 0.5%, under RCP4.5 a decrease of similar magnitude is assessed (-0.6%); finally, under RCP8.5, the decrease slightly exceeds 1% with a maximum decrease in October (about 7% under an increase in temperature of about 3.2°C).

Similar bias corrections were carried out for Lisbon and Faro. The detailed results given in Appendix A also highlight the importance of performing bias corrections.

5 CARBONATION EFFECTS UNDER A CHANGING CLIMATE

5.1 Parameters adopted for the analysis

This section provides the calculation of carbonation depths of reinforced concrete structures in Portugal for two distinct periods: the period 1981-2018, based on the historic climate data described in the previous section, is used as reference; the period 1981-2100 is used to provide assessments about future evolutions under the potential impact of climate change. Of course, as the climate simulation chains has been bias-adjusted over the reanalysis data for the time span 1981-2010 (Section 4), in this period the two evaluations tend to be overlapped in terms of average value but not in terms of month-by-month evolution. The assessment is conducted for several locations geographically distributed in the three different districts illustrated in Figure 2. The main outcome of the computations is the carbonation depth and is based on the model described in Section 3, Equation (4), considering the conditions described in Section 4, and the parameters listed in Table 3. Since the study will mainly focus on assessing the effects of external environmental actions on carbonation depths, only one ordinary concrete fabricated with Portland cement was considered.

Table 3: Parameters used in the calculation of carbonation depth

Parameter	Value and observations	References
D_1	6×10^{-4} cm²/s	(Talukdar et al, 2012b)
k_{site}	1.14 (urban exposure, Porto and Lisbon districts) 1.05 (rural exposure, Faro district)	(Peng and Stewart, 2014)
t_0	1 year	(Talukdar et al, 2012b)
n_d	0.24	(Yoon et al, 2007)
n_m	0 (sheltered outdoor exposure)	(Duracrete, 2000)
E	40 kJ/mol	(Kada-Benameur et al, 2000)
w/c	0.5	–
C_e	300 kg/m³	–
t_{const}	1981	–

5.2 Assessment of carbonation depth for the historic/current period

The carbonation depth over the current period (1981-2018) is provided in the following paragraphs, for a concrete structure assumed to be built in 1981. The assessment of the carbonation depth over time for the district of Porto is illustrated in Figure 7a, for the 4 locations shown in Figure 2b. For each one, the closest grid point extracted from ERA5-land grid is assumed as the best proxy. As observed from Figure 7a, the variation of the carbonation depth, over the current period, is almost negligible for the 4 locations. Although the value obtained for V.N. Gaia is slightly higher than the other values. This small variation indicates that the environmental exposure conditions are quite similar for all 4 locations. The findings could be partly due, as reported before, by the adoption of ERA5-land that could underestimate intra-urban variations.

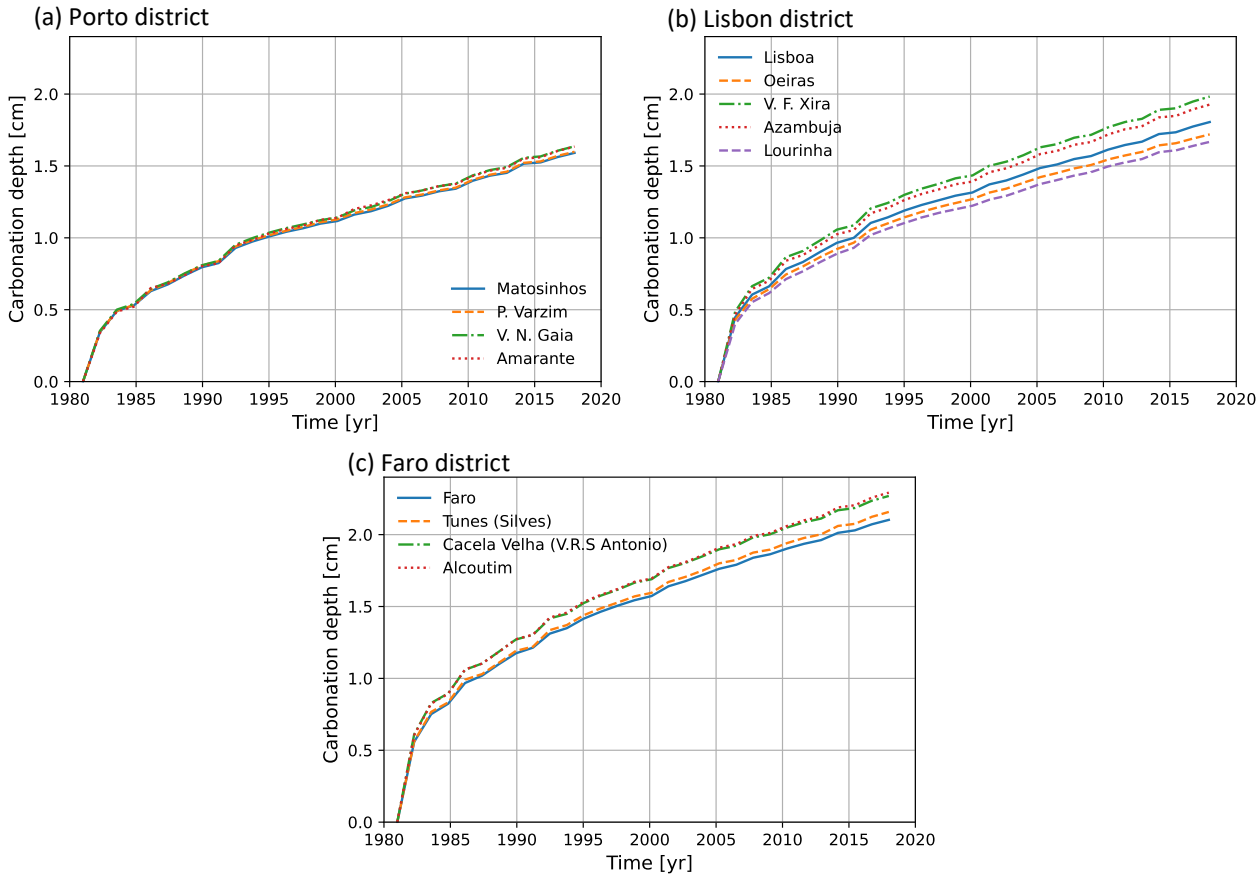

Figure 7: Variation of carbonation depths in the districts of (a) Porto, (b) Lisbon, and (c) Faro

For the district of Lisbon, the assessment of the carbonation depth over time is illustrated in Figure 7b, for the 5 grid points identified in Figure 2c. In this case, the carbonation depth, over the current period, varies from a minimum value of 1.67 cm, in Lourinhã, to a maximum value of 1.98 cm, in V.F. Xira. In all cases, the values are referring to year 2018. Figure 7c illustrates the assessment of the carbonation depth over time for the district of Faro, for the 4 grid points identified in Figure 2d. In this district, the carbonation depth varies from a minimum value of 2.10 cm, in Faro, to a maximum value of 2.29 cm, in Alcoutim. Likewise, in all cases, the values are referring to year 2018. The results on Figure 7 illustrate about importance of considering specific exposure conditions at different scales. While the variations are almost negligible for the locations in the Porto district, they could have a great impact on durability assessments for Lisbon and Faro districts.

To better understand how the carbonation depths are influenced by time-dependent external variations of CO_2 concentration, temperature, and relative humidity, Figure 8 provides the carbonation depths for 5 carbonation models and for 3 places:

- The first model (blue lines) considers that CO_2 concentration in the air is constant and neglects effects of temperature and RH variations (Equation 1).
- The second one (orange lines) supposes that CO_2 concentration in the air increases, as shown in Figure 4, but neglects effects of temperature and RH variations. Hence, the integral inside Equation 4 becomes $\int C_{CO_2}(t)dt$.
- The third one (green lines) accounts for variations of CO_2 concentration in the air and temperature. Therefore, the integral inside Equation 4 becomes $\int f_T(t)C_{CO_2}(t)dt$.
- The four one (red lines) considers variations of CO_2 concentration in the air and RH. Then, the integral inside Equation 4 is $\int f_{RH}(t)C_{CO_2}(t)dt$.
- The last one (purple lines) accounts for time-dependency of all factors (Equation 4).

It is observed that the predictions of the two first models give the same results because they neglect environmental variations that are specific for each place. Larger carbonation depths are expected for the second model because it accounts for the increase of CO_2 concentration due to climate change. The lower carbonation depths are observed for the locations in the districts of Porto and Lisbon when considering all

environmental effects (Equation 4). This is explained by the fact that average temperatures are lower than $T_{ref} = 20$ ºC and relative humidity are larger than 0.65 for both places (Figure 3). Therefore, the factors $f_T(t)$ and $f_{RH}(t)$ will be mostly lower than one (Figure 1) by reducing the CO_2 diffusion coefficient. These environmental effects are larger for the location in the Porto district. A different behavior is observed for the district of Faro that is characterized by a relative humidity that is within the range of values where carbonation is accelerated [0.25, 0.65] (Figure 1). The average annual temperature is a little bit lower than T_{ref} (Figure 3); this counteracts the effects of relative humidity. These results stress the necessity of considering environmental inputs at a correct scale in the lifetime assessment.

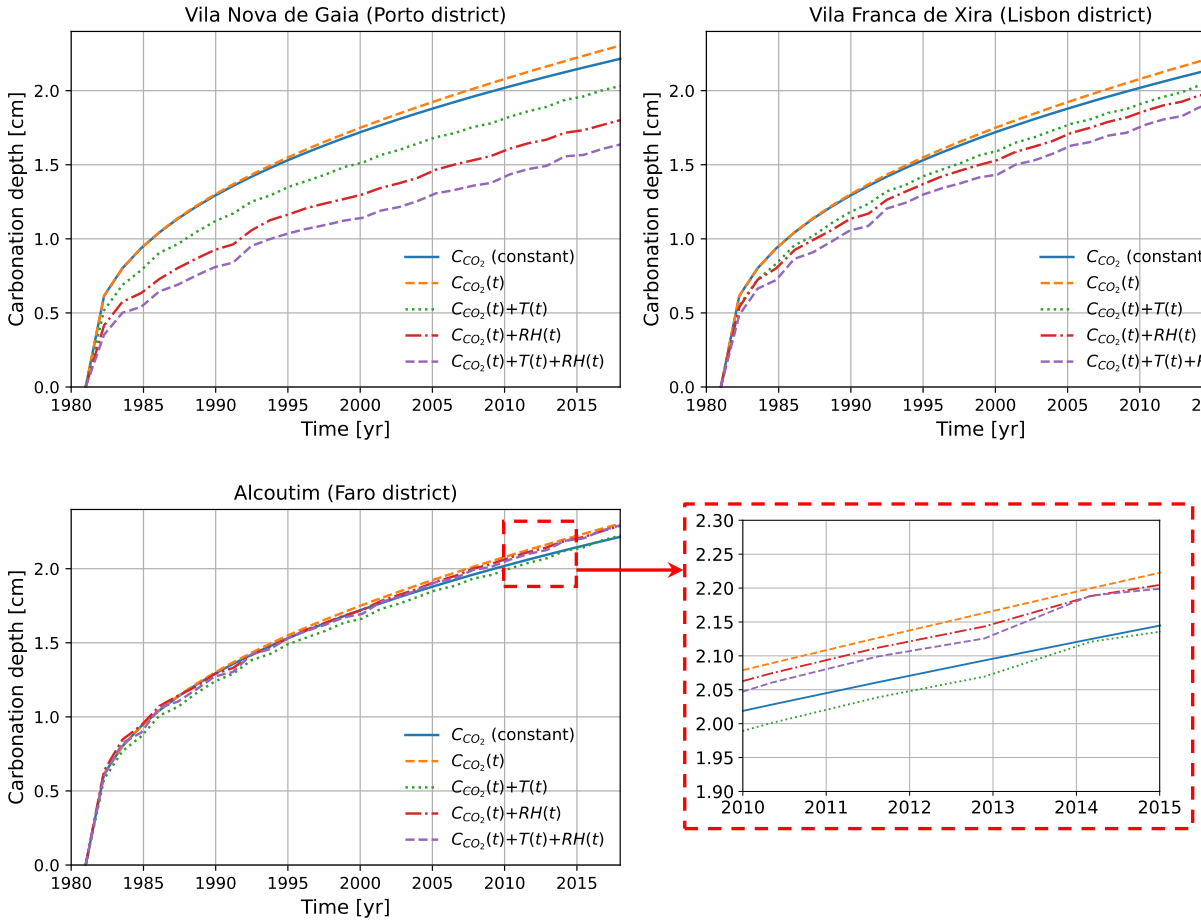

Figure 8: Carbonation depths when considering time-dependency of CO_2 concentration, temperature, and relative humidity for the districts of Porto, Lisbon, and Faro

The mean value of the carbonation depth, over time, for each district is illustrated in Figure 9. The carbonation depth in the south of the country is higher (about 32%) than in the northern part of the country. This was already expected from results in Figures 7 and 8, as the RH in the southern part of the country is lower than in the northern part. In general terms, it is important to highlight that inter-district variability in atmospheric patterns could be underestimated by using ERA5land with a horizontal resolution of 9km.

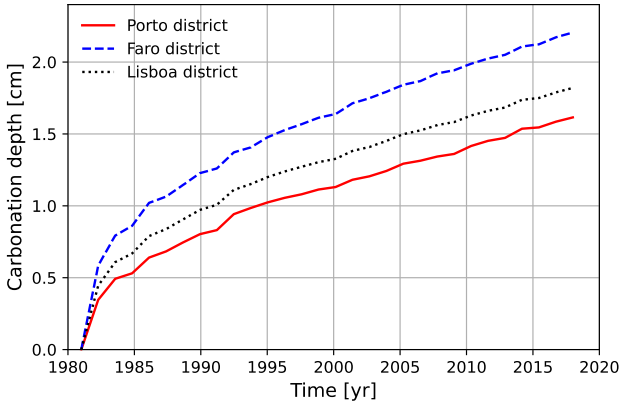

Figure 9: Mean variation of carbonation depth in the three districts

5.3 Raw versus bias corrected climate data

The carbonation depths represented in Figures 7 to 9 are based on observed data over the historic period (ERA5-L). To show the importance of bias correction of climate data, the carbonation depth was calculated for the same period, based on raw data (Figure 10a) and bias corrected data (Figure 10b). The two climate simulation chains indicated in Table 1 are considered in this analysis: ICHEC-EC-EARTH and MPI-M-MPI-ESM-LR. When comparing the results obtained by using raw data, it is observed that there are significant errors with respect to the carbonation depths computed using the reference values (ERA5-L). This could lead, for example, to an over estimation of ~7 years of the time to corrosion initiation for Faro, if the steel bar is placed at 2 cm. In contrast, Figure 10b shows that the errors between the results obtained with ERA5-L and bias corrected data are significantly reduced. Therefore, bias correction becomes essential when assessing the long-term performance of infrastructure assets under a changing climate.

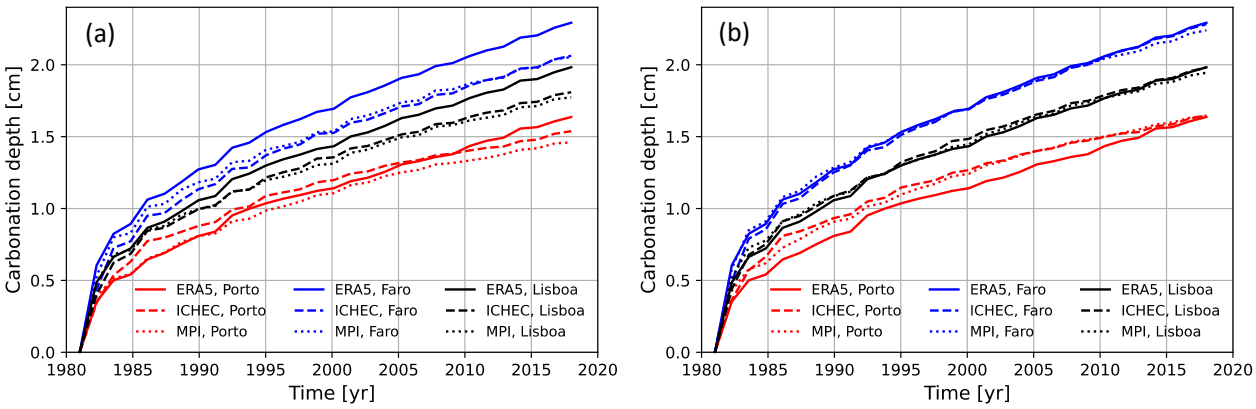

Figure 10: Effect of bias correction on the carbonation depths for the reference points: (a) raw, and (b) bias corrected data

5.4 Assessment of carbonation depth considering climate projections

In this case, the carbonation depths are estimated for the period 1981 – 2100, considering RCP2.6, RCP4.5 and RCP8.5 scenarios. Climate projections for the different locations were collected and bias corrected according to the procedure described in section 4. The calculation is performed for the two climate simulation chains indicated in Table 1: ICHEC-RCA4 and MPI-RCA4.

Figure 11 illustrates the carbonation depths for the ICHEC-RCA4 and MPI-RCA4 CSCs and the three reference grid points indicated in Figure 2: district of Porto (north), district of Lisbon (middle), and district of Faro (south). As already observed from the previous calculations, the carbonation depths in the southern part of the country (Faro) remain higher than in the northern part for long-term assessment. In this case, the

difference for the year 2100 is about: (i) +35% for RCP 8.5 and +38% for RCP 2.6 (ICHEC-RCA4) and (ii) +37% for RCP 8.5 and +41% for RCP 2.6 (MPI-RCA4).

Carbonation depths values in Figure 11 for both simulation chains are very close and the trends for each place and climate change scenario are in overall consistent. This result is expected because each simulation chain considers specific driving methods to generate the data e.g., ensemble, data source, Institution, Jet stream, influence, aerosols, forcing, initial state of run, etc. (Habeeb and Bastidas-Arteaga, 2022). The relative differences between ICHEC-RCA4 and MPI-RCA4 estimated by taking as reference the MPI-RCA4 simulation chain are also provided in Figure 11 (bottom). It is observed that the relative differences are mostly positive indicating that the carbonation depths provided by the climate model MPI-RCA4 are slightly higher than those given by ICHEC-RCA4. It is usually hard to identify the reasons for such variations; indeed, also if the climate simulation chains share the same regional climate models, the differences cannot be due only to GCM because parameters, the choice of specific parametrizations or the tuning process play a significant role. Nevertheless, in general terms, ECS for MPI-M-MPI-ESM-LR acting as GCM in the second case is slightly higher than that for ICHEC (3.6° vs 3.3°) probably entailing higher increase in temperature and then higher values of carbonation depth.

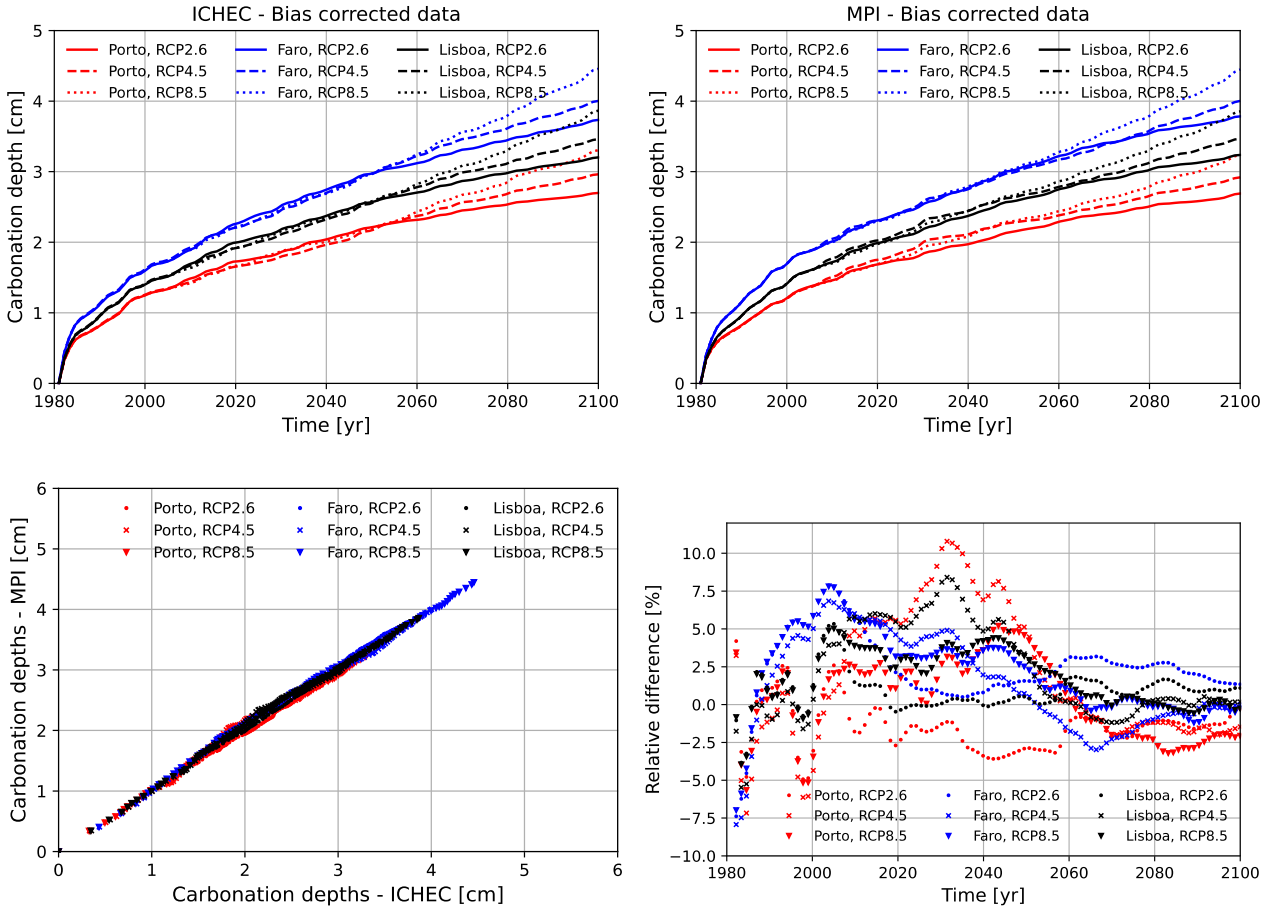

Figure 11: Carbonation depths and relative difference for both climate simulation chains using bias corrected data

In the following, the same calculations are performed but using raw data. In this case, the results are presented in Figure 12, for climate models ICHEC-RCA4 and MPI-RCA4, respectively. The general carbonation trends for the three locations do not change. In accordance with the results presented in Section 5.2, it is observed that, for long term projections, the values of the carbonation depths obtained when using raw data are always underestimating, for all locations and for all RCPs.

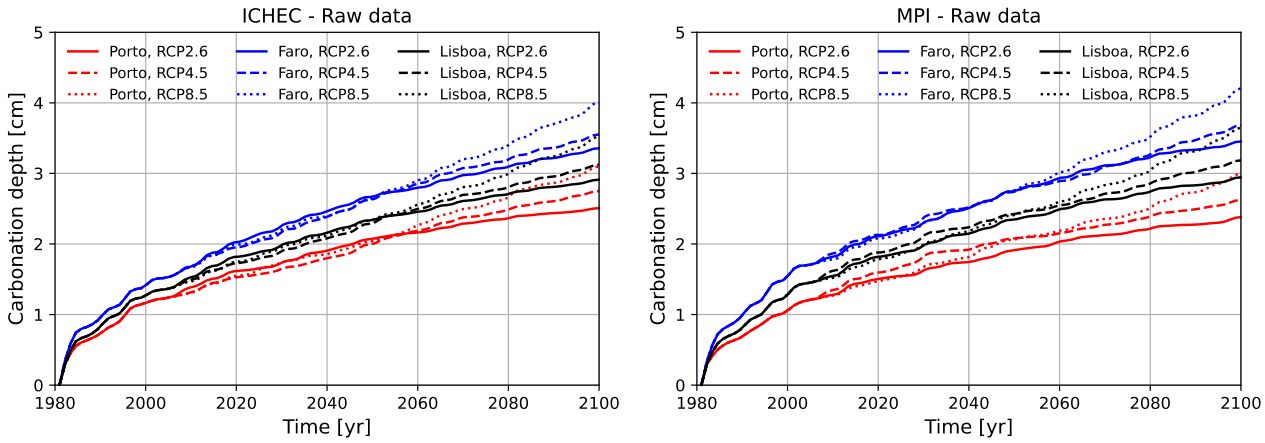

Figure 12: Carbonation depths for both climate simulation chains and raw data

The times to corrosion initiation, computed by considering a concrete cover of 3 cm, are provided in Table 4. All locations and scenarios were considered in the analysis. Both simulation chains and bias-corrected data were used in the simulations. In accordance with the carbonation depths depicted in Figure 11, it was found that corrosion initiation starts first in Faro, followed by Lisboa and Porto. For most part of locations, corrosion starts earlier for the more pessimistic scenario (RCP 8.5). This trend was not clearly observed for Faro because for this location the main effects of climate change start in by 2050 where the carbonation depth is very close to the concrete cover (Figure 11).

Table 4: Times to corrosion initiation for a concrete cover of 3 cm

Simulation chain (only bias corrected)	Porto			Faro			Lisboa		
	RCP2.6	RCP4.5	RCP8.5	RCP2.6	RCP4.5	RCP8.5	RCP2.6	RCP4.5	RCP8.5
MPI-RCA4	>2100	>2100	2091	2048	2050	2047	2078	2073	2066
ICHEC-RCA4	>2100	>2100	2085	2051	2050	2050	2080	2071	2067

As further observed from Table 4, there are also some differences in the time to corrosion initiation between both simulation chains. Therefore, it is important to include several simulation chains to account also for the uncertainties related with climate predictions. The predictions could be also improved by using a probabilistic approach to consider all sources of uncertainty in the problem.

6 CONCLUSIONS AND FURTHER WORK

This paper presented an approach for multi-regional assessment of concrete carbonation under changing climate. Depending on the scale of the analysis (e.g., European, National, regional, etc.), the approach provides the main procedures to reduce durability assessment errors: selection of climate change scenarios, simulation chains, and bias correction. The approach was applied for short and long-term estimation of carbonation depths of reinforced concrete structures located in three Portuguese regions (districts of Porto, Lisboa and Faro). The main conclusions of this study are summarized as follows:

- The analysis of historic and future climate conditions allows to identify specific environments that would affect in a different way the durability of reinforced concrete structures. This analysis allowed for example to identify that, even without climate change, the range of variation of relative humidity for Faro increased carbonation rates in comparison with the other two districts. This kind of observation for a particular place was very similar. This highlights the consistency between the main driving methods for both simulation chains when predicting future climate conditions.
- The results of carbonation depths cannot be generalized at a district scale. The carbonation depths for the Porto district were very close for all locations; therefore, it could be wrongly assumed, based on this finding, that the results for one reference point could be used at the district scale. The results

for the other two districts show that microclimate conditions could significantly affect lifetime assessments.

- Bias correction is essential to reduce errors in lifetime assessments. In the short term (1981-2018) it was possible to assess that raw data results on wrong estimations in comparison with representative climate conditions provided by ERA5-L. These differences were also observed in long term (1981-2100) assessments where using raw data conducted to relative errors from 5 to 14%. In this study, raw data conducted to over estimations of the carbonation depth; however, other behaviours could be observed for other locations.
- Climate change will shorten the time to corrosion initiation. The effects differ for each location but in overall are remarkable after 2050 and are larger for the more pessimistic scenario (RCP 8.5). Consequently, a regional assessment as the proposed on this study would be helpful to identify the most affected places and to plan inspection and maintenance actions.

Further work is this area should be addressed to:

- Consider more advanced carbonation models, and/or the interaction between chloride ingress and carbonation (Guo et al, 2022), to improve corrosion initiation assessment.
- Assess and study the carbonation under a changing climate when using more sustainable cementitious materials (Lippiatt et al 2020; Bennett et al 2022; Neves and Brito, 2022).
- Study the effect of repair/retrofit reinforced concrete structures (Truong et al, 2022) as well as the computation of the cost-effectiveness of these actions under a changing climate (Bastidas-Arteaga, 2021).
- Apply the approach to study other deterioration mechanisms as chloride induced corrosion or corrosion propagation in concrete or to consider other construction materials.
- Consider more simulation chains and the different sources of uncertainty of the problem using a full probabilistic approach.

DECLARATION OF COMPETING INTEREST

The authors declare that they have no known competing financial interests or personal relationships that could have appeared to influence the work reported in this paper.

ACKNOWLEDGMENTS

E.B.-A. contribution was carried out in the framework of the Strengthening the Territory's Resilience to Risks of Natural, Climate and Human Origin (SIRMA) project, which is co-financed by the European Regional Development Fund (ERDF) through INTERREG Atlantic Area Program with application code: EAPA_826/2018. The sole responsibility for the content of this publication lies with the authors. It does not necessarily reflect the opinion of the European Union. Neither the INTERREG Europe program authorities are responsible for any use that may be made of the information contained therein.

We acknowledge the World Climate Research Programme's Working Group on Regional Climate, and the Working Group on Coupled Modelling, former coordinating body of CORDEX and responsible panel for CMIP5. We also thank the climate modelling groups (listed in Table 1 of this paper) for producing and making available their model output. We also acknowledge the Earth System Grid Federation infrastructure, an international effort led by the U.S. Department of Energy's Program for Climate Model Diagnosis and Intercomparison, the European Network for Earth System Modelling and other partners in the Global Organisation for Earth System Science Portals (GO-ESSP).

ERA5Land data have been obtained by Copernicus Climate Change Service Information and downloaded from the Copernicus Climate Change Service (C3S) Climate Data Store.

APPENDIX A: BIAS CORRECTION RESULTS FOR LISBON AND FARO

Figure A.1 shows the bias correction evaluations for Lisbon test case. In general terms, adopting ICHEC-RCA4, the yearly mean increases are comparable: 0.8°C, 1.7°C and 3.2°C under the three scenarios; moreover, the maximum values are assessed for the summer season (2.2°C in July for RCP4.5, 4.5 for RCP8.5) or soon after it (1.1°C in September for RCP2.6). Lower increases are expected by considering MPI-RCA4: 0.5°C under RCP2.6, 1.4°C under RCP4.5 and about 3°C for RCP8.5 (maximum value 3.8°C in September). For what concerns relative humidity, by considering ICHEC-RCA4, similar findings are retrieved with the larger mean decrease expected under RCP8.5 (-2.2%; max values in May about -7%). On the other side, for MPI-RCA4, again, the larger decrease is expected under RCP8.5 with a value about equal to -3% at yearly scale but a peak in October (-9% driven by an increase in temperature of about 3.5°C). Under less severe RCPs, yearly variations in RH are close to ±1%.

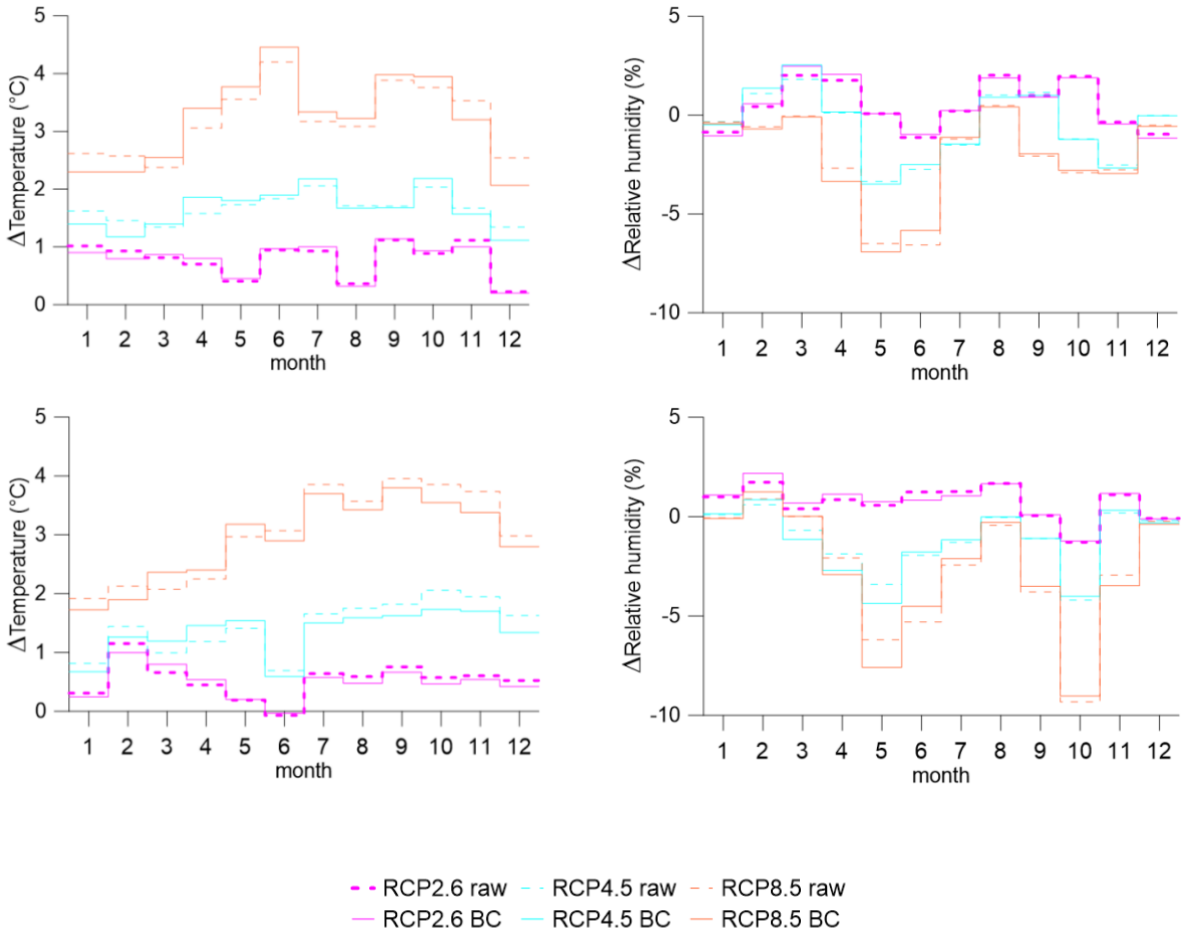

Figure A.1: Lisbon test case. Climate anomalies between the period 2071-2100 and the reference period 1981-2010 under RCP2.6 (magenta), RCP4.5(cyan), RCP8.5(orange) as returned by CSCs raw (dashed line) and BC (continuous line); for ICHEC-RCA4 (first row) and MPI-RCA4 (second row); for temperature (first column) and relative humidity (second column).

Finally, Figure A.2 reports the assessed anomalies for Faro pilot case. For ICEC-RCA4 the findings are similar to those previously discussed. However, it is worth to point out how, under RCP8.5, the yearly increase slightly exceeds 3.5°C with a peak value in June of about 5°C (4.6°C in September). By considering MPI-RCA4 similar findings are retrievable: the yearly anomaly value is equivalent but with a peak value in June of about 5.3°C. Such patterns also regulate the variations of relative humidity for the two CSCs with evident decreases (up to -10%) in the Spring season.

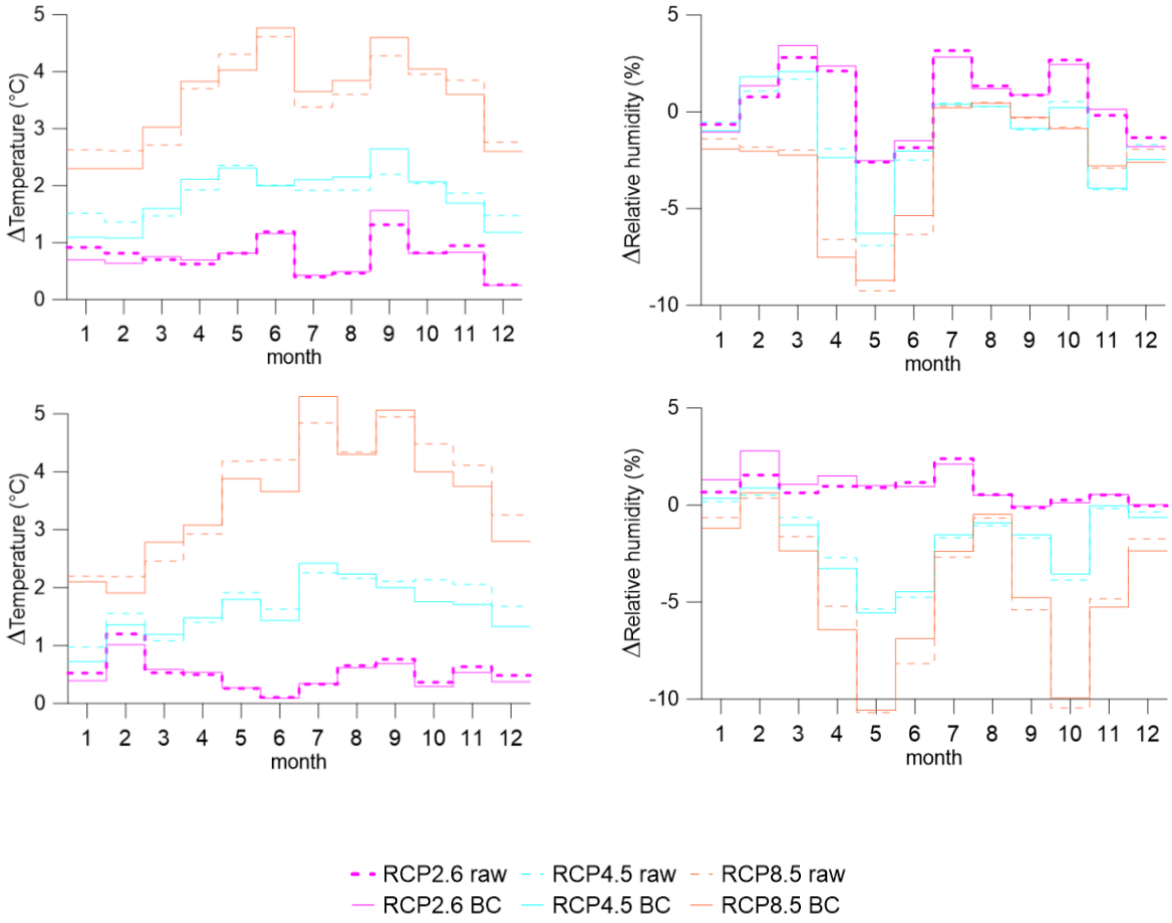

Figure A.2: Faro test case. Climate anomalies between the period 2071-2100 and the reference period 1981-2010 under RCP2.6 (magenta), RCP4.5(cyan), RCP8.5(orange) as returned by CSCs raw (dashed line) and BC (continuous line); for ICHEC-RCA4 (first row) and MPI-RCA4 (second row); for temperature (first column) and relative humidity (second column).

BIBLIOGRAPHY

AL-Ameeri, A., Rafiq, M., Tsioulou, O., & Rybdylova, O. (2021). Impact of climate change on the carbonation in concrete due to carbon dioxide ingress: Experimental investigation and modelling. Journal of Building Engineering, 44, 102594.

APA, Agência Portuguesa do Ambiente, https://apambiente.pt/clima/inventario-nacional-de-emissoes-por-fontes-e-remocao-por-sumidouros-de-poluentes-atmosfericos <Accessed on 25/11/2021>.

Balsamo, G., Beljaars, A., Scipal, K., Viterbo. P., van den Hurk, B., Hirsch, M., Betts, A. (2009). A revised hydrology for the ECMWF model: verification from field site to terrestrial water storage and impact in the Integrated Forecast System. J Hydrometeorol 10: 623–643. https://doi.org/10.1175/2008JHM1068.1.

Bastidas-Arteaga, E. (2021). Towards Climate Change Adaptation of Existing and New Deteriorating Infrastructure. 18th International Probabilistic Workshop, Lecture Notes in Civil Engineering, J. C. Matos, P. B. Lourenço, D. V. Oliveira, J. Branco, D. Proske, R. A. Silva, and H. S. Sousa, eds., 39–51. Cham: Springer International Publishing.

Bell, B., Hersbach, H., Berrisford, P., Dahlgren, P., Horányi, A., Muñoz Sabater, J., Nicolas, J., Radu, R., Schepers, D., Simmons, A., Soci, C., Thépaut, J-N. (2020). ERA5 monthly averaged data on pressure levels from 1950 to 1978 (preliminary version). Copernicus Climate Change Service (C3S) Climate Data Store (CDS). (Accessed on < 24-3-2021 >), https://cds.climate.copernicus-climate.eu/cdsapp#!/dataset/reanalysis-era5-pressure-levels-monthly-means-preliminary-back-extension?tab=overview.

Bennett, B., Visintin, P., Xie, T. (2022). Global warming potential of recycled aggregate concrete with supplementary cementitious materials. Journal of Building Engineering, 52: 104394. https://doi.org/10.1016/j.jobe.2022.104394.

Breugem, W., Hazeleger W., Haarsma, R. (2007). Mechanisms of northern tropical Atlantic variability and response to CO2 doubling. Journal of Climat , vol 20(11): 2691-2705.

Casanueva A, Herrera S, Iturbide M, Lange S, Jury M et al (2020zz) Testing bias adjustment methods for regional climate change applications under observational uncertainty and resolution mismatch. Atmos Sci Lett 21:e978. https://doi.org/10.1002/asl.978

Chen, G., Lv, Y., Zhang, Y., & Yang, M. (2021). Carbonation depth predictions in concrete structures under changing climate condition in China. Engineering Failure Analysis, 119, 104990.

Cole, I., Paterson, D. (2010). Possible effects of climate change on atmospheric corrosion in Australia. Corrosion Engineering, Science and Technology, 45:1, 19-26, https://doi.org/10.1179/147842209X12579401586483.

Coppola E., Nogherotto R., Ciarlò J.M., Giorgi F., van Meijgaard E., Kadygrov N., Iles C., Corre L., Sandstad M., Somot S., Nabat P., Vautard R., Levavasseur G., Schwingshackl C., Sillmann J., Kjellström E., Nikulin G., Aalbers E., Lenderink G., Christensen O.B., Boberg F., Lund Sørland S., Demory M.-E., Bülow K., Teichmann C., Warrach-Sagi K., Wulfmeyer V. (2021). Assessment of the European climate projections as simulated by the large EURO-CORDEX regional and global climate model ensemble. Journal of Geophysical Research – Atmospheres, doi: 10.1029/2019JD032356.

de Larrard, F. (1999). Concrete mixture proportioning: a scientific approach, E & FN Spon. ed. London.

Dee, D., Uppala, S., Simmons, A., Berrisford, P., Poli, P., Kobayashi, S., Andrae, U., Balmaseda, M., Balsamo, G., Bauer, P., Bechtold, P., Beljaars, A., van de Berg, L., Bidlot, J., Bormann, N., Delsol, C., Dragani, R., Fuentes, M., Geer, A., Haimberger, L., Healy, S., Hersbach, H., Hólm, E., Isaksen, L., Kållberg, P., Köhler, M., Matricardi, M., McNally, A., Monge-Sanz, B., Morcrette, J., Park, B., Peubey, C., de Rosnay, P., Tavolato, C., Thépaut, J., Vitart, F. (2011). The ERA-Interim reanalysis: configuration and performance of the data assimilation system. Q J Roy Meteor Soc 137:553–597. https://doi.org/10.1002/qj.828.

Dosio, A. (2016). Projections of climate change indices of temperature and precipitation from an ensemble of bias-adjusted highresolution EURO-CORDEX regional climate models. Journal of Geophysical Research—Atmospheres, 121, 5488–5511. https:// doi.org/10.1002/2015JD024411.

DuraCrete (2000). Statistical quantification of the variables in the limit state functions. DuraCrete—probabilistic performance based durability design of concrete structures. EU—brite EuRam III. Contract BRPR-CT95-0132. Project BE95-1347/R9.

Ekolu, S. (2020). Implications of global CO2 emissions on natural carbonation and service lifespan of concrete infrastructures–Reliability analysis. Cement and Concrete Composites, 114, 103744.

fib (2006). Model Code for Service Life Design. Lausanne: Fib Bulletin 34.

Guo, B., G. Qiao, P. Han, Z. Li, and Q. Fu. (2022). Effect of natural carbonation on chloride binding behaviours in OPC paste investigated by a thermodynamic model. Journal of Building Engineering, 49: 104021. https://doi.org/10.1016/j.jobe.2022.104021.

Habeeb, B., Bastidas-Arteaga, E. (2022). Climate change indicators dataset for coastal locations of the European Atlantic area. Data in Brief, 43 (2022) 108339, https://doi.org/10.1016/j.dib.2022.108339

Hersbach, H., Bell, B., Berrisford, P., Biavati, G., Horányi, A., Muñoz Sabater, J., Nicolas, J., Peubey, C., Radu, R., Rozum, I., Schepers, D., Simmons, A., Soci, C., Dee, D., Thépaut, J-N. (2019). ERA5 monthly averaged data on pressure levels from 1979 to present. Copernicus Climate Change Service (C3S) Climate Data Store (CDS). (Accessed on < 24-3-2021>), 10.24381/cds.6860a573.

IPCC (2014). Climate Change 2014: Synthesis Report. Contribution of Working Groups I, II and III to the Fifth Assessment Report of the Intergovernmental Panel on Climate Change. Geneva, Switzerland (151 pp.).

IPCC (2021). Summary for Policymakers. In: Climate Change 2021: The Physical Science Basis. Contribution of Working Group I to the Sixth Assessment Report of the Intergovernmental Panel on Climate Change [MassonDelmotte, V., P. Zhai, A. Pirani, S.L. Connors, C. Péan, S. Berger, N. Caud, Y. Chen, L. Goldfarb, M.I. Gomis, M. Huang, K. Leitzell, E. Lonnoy, J.B.R. Matthews, T.K. Maycock, T. Waterfield, O. Yelekçi, R. Yu, and B. Zhou (eds.)]. Cambridge University Press, Cambridge, United Kingdom and New York, NY, USA, pp. 3−32, doi:10.1017/9781009157896.001.

IPMA, Instituto Português do Mar e da Atmosfera, https://www.ipma.pt/pt/educativa/tempo.clima/ <Accessed on 14/01/2022>.

Jacob, D., Teichmann, C., Sobolowski, S. et al. (2020). Regional climate downscaling over Europe: perspectives from the EURO-CORDEX community. Reg Environ Change 20, 51. https://doi.org/10.1007/s10113-020-01606-9.

Kada-Benameur, H., Wirquin, E., & Duthoit, B. (2000). Determination of apparent activation energy of concrete by isothermal calorimetry. Cement and Concrete Research, 30, 301– 305.

Larrard, T., Bastidas-Arteaga, E., Duprat, F., Schoefs, F. (2014). Effects of Climate Variations and Global Warming on the Durability of RC Structures Subjected to Carbonation. Civil Engineering and Environmental Systems, https://doi.org/10.1080/10286608.2014.913033.

Li, D., Yang, L., Lam, J. (2012). Impact of climate change on energy use in the built environment in different climate zones – A review. Energy, Volume 42, Issue 1, 103-112, ISSN 0360-5442, https://doi.org/10.1016/j.energy.2012.03.044.

Lippiatt, N., Ling, T., Pan, S. (2020). Towards carbon-neutral construction materials: Carbonation of cement-based materials and the future perspective. Journal of Building Engineering, 28: 101062. https://doi.org/10.1016/j.jobe.2019.101062.

Londhe, S., Kulkarni, P., Dixit, P., Silva, A., Neves, R., de Brito, J. (2021). Predicting carbonation coefficient using Artificial neural networks and genetic programming. Journal of Building Engineering, 39: 102258. https://doi.org/10.1016/j.jobe.2021.102258.

Maraun, D. (2016). Bias Correcting Climate Change Simulations - a Critical Review. Curr Clim Chang Reports, doi:10.1007/s40641-016-0050-x.

Maraun, D., Shepherd, T., Widmann, M. et al. (2017). Towards process-informed bias correction of climate change simulations. Nature Clim Change 7, 764–773. https://doi.org/10.1038/nclimate3418.

Meehl, G., Senior, C., Eyring, V., Flato, G., Lamarque, J.-F.,Stouffer, R., Taylor, K., Schlund, M. (2020). Context for interpreting equilibrium climate sensitivity and transient climate response from the CMIP6 Earth system models, Sci. Adv., 6, eaba1981, https://doi.org/10.1126/sciadv.aba1981.

Mizzi, B., Wang, Y., Borg, R. (2018). Effects of climate change on structures; analysis of carbonation-induced corrosion in Reinforced Concrete Structures in Malta. In IOP Conference Series: Materials Science and Engineering (Vol. 442, No. 1, p. 012023). IOP Publishing.https://doi.org/10.1088/1757-899X/442/1/012023.

Muñoz-Sabater, J., (2019). ERA5-Land hourly data from 1981 to present. Copernicus Climate Change Service (C3S) Climate Data Store (CDS). DOI 10.24381/cds.e2161bac.

Neves, R., de Brito, J. (2022). Estimated service life of ordinary and high-performance reinforced recycled aggregate concrete. Journal of Building Engineering, 46: 103769. https://doi.org/10.1016/j.jobe.2021.103769.

Oreskes, N., Stainforth, D., Smith, L. (2010). Adaptation to Global Warming: Do Climate Models Tell Us What We Need to Know? Philosophy of Science, 77(5), 1012–1028. https://doi.org/10.1086/657428.

Page, C., Short, N., El Tarras, A. (1981). Diffusion of chloride ions in hardened cement pastes. Cem. Concr. Res. 11, 395–406. https://doi.org/10.1016/0008-8846(81)90111-3.

Parker, W. (2013). Ensemble modeling, uncertainty and robust predictions. WIREs Clim. Change 4, 213–223.

Peng, L., Stewart, M. (2014). Spatial time-dependent reliability analysis of corrosion damage to RC structures with climate change. Magazine of Concrete Research, 66(22), 1154–1169. https://doi-org.tudelft.idm.oclc.org/10.1680/macr.14.00098.

Ravahatra, N., Bastidas-Arteaga, E., Schoefs, F., de Larrard, T., Duprat, F. (2019). Probabilistic and sensitivity analysis of analytical models of corrosion onset for reinforced concrete structures. European Journal of Environmental and Civil Engineering, 1–30. https://doi.org/10.1080/19648189.2019.1591307.

Saha, M., Eckelman, M. (2014). Urban scale mapping of concrete degradation from projected climate change. Urban Climate, 9, 101–114. https://doi.org/10.1016/j.uclim.2014.07.007.

Sanderson, B., Knutti, R. (2012). On the interpretation of constrained climate model ensembles, Geophys. Res. Lett., 39, L16708, doi:10.1029/2012GL052665.

Schiessl, P., Helland, S., Gehlen, C., Nilsson, L.-O. (2005). Model Code for Service Life Design (MC-SLD), in: Fib Symposium, Structural Concrete and Time. La Plata, p. 10.

Stewart, M., Teply, B., Kralova, H. (2002). The effect of temporal and spatial variability of ambient carbon dioxide concentrations on carbonation of RC structures. In: 9th international conference on durability of building materials and components. CSIRO. Paper 246.

Stewart, M., Wang, X., Nguyen, M. (2011). Climate change impact and risks of concrete infrastructure deterioration. Eng. Struct. 33, 1326–1337. https://doi.org/10.1016/j.engstruct.2011.01.010.

Sudret, B., Defaux, G., Pendola, M. (2007). Stochastic evaluation of the damage length in RC beams submitted to corrosion of reinforcing steel. Civ Eng Environ Syst, 24 (2) (2007), pp. 165-178.

Switanek, M., Troch, P., Castro, C., Leuprecht, A., Chang, H.-I., Mukherjee, R., Demaria, E.M.C. (2017). Scaled distribution mapping: a bias correction method that preserves raw climate model projected changes. Hydrology and Earth System Sciences, 21, 2649–2666. https://doi.org/10.5194/hess-21-2649-2017.

Talukdar, S., Banthia, N. (2013). Carbonation in concrete infrastructure in the context of global climate change: development of a service lifespan model. Construction and Building Materials, 40,775–782. https://doi.org/10.1016/j.conbuildmat.2012.11.026.

Talukdar, S., Banthia, N., Grace, J. (2012b). Carbonation in concrete infrastructure in the context of global climate change – Part 1: Experimental results and model development. Cement and Concrete Composites, 34 (8): 924–930. https://doi.org/10.1016/j.cemconcomp.2012.04.011.

Talukdar, S., Banthia, N., Grace, J., Cohen, S. (2012a). Carbonation in concrete infrastructure in the context of global climate change: Part 2– Canadian urban simulations. Cement and Concrete Composites, 34(8), 931–935. https://doi.org/10.1016/j.cemconcomp.2012.04.012.

Tebaldi, C., Knutti, R. (2007). The use of the multi-model ensemble in probabilistic climate projections. Philosophical Transactions of the Royal Society A: Mathematical, Physical and Engineering Sciences, 365(1857), 2053–2075. doi:10.1098/rsta.2007.2076.

Trivedi, N., Venkatraman, M., Chu, C., Cole, I. (2014). Effect of climate change on corrosion rates of structures in Australia. Climate change 124, 133-146, https://doi.org/10.1007/s10584-014-1099-y.

Truong, Q., El Soueidy, C., Li, Y., Bastidas-Arteaga, E. (2022). Probability-based maintenance modeling and planning for reinforced concrete assets subjected to chloride ingress. Journal of Building Engineering, 54: 104675. https://doi.org/10.1016/j.jobe.2022.104675.

UKCIP (2005). Measuring Progress—Preparing for Climate Change Through the UKCIP 〈 http://www.ukcip.org.uk/resources/publications/documents/100.pdf〉.

USAID (2014). A review of downscaling methods for climate change projections. U.S. Agency for International Development, Washington https://www.asocam.org/sites/default/files/publicaciones/files/55ec0a669288f39b71512b6934a43980.pdf

van Vuuren, D., Edmonds, J., Kainuma, M. et al. (2011). The representative concentration pathways: an overview. Climatic Change 109, 5. https://doi.org/10.1007/s10584-011-0148-z.

Wilby, R. (2007). A Review of Climate Change Impacts on the Built Environment. Built Environment. 33. 31-45, 10.2148/benv.33.1.31.

Wilby, R., Dessai, S. (2010). Robust adaptation to climate change. Weather, 65: 180-185. https://doi.org/10.1002/wea.543.

Wyser, K., van Noije, T., Yang, S., von Hardenberg, J., O'Donnell, D., Döscher, R. (2020). On the increased climate sensitivity in the EC-Earth model from CMIP5 to CMIP6, Geosci. Model Dev., 13, 3465–3474, https://doi.org/10.5194/gmd-13-3465-2020.

Yoon, I., Çopuroğlu, O., Park, K. (2007). Effect of global climatic change on carbonation progress of concrete. Atmos. Environ. 41, 7274–7285. https://doi.org/10.1016/j.atmosenv.2007.05.028.